Research article

Intracellular Ca²⁺ rhythmic activity in human glioblastoma multiforme cells

Células de glioblastoma multiforme humano generan actividad rítmica de calcio intracelular

[1]Diana Monge-Sanchez [iD] , [2]Javier Alejandro Aguirre-Alegria, [1]Denisse García-Villa, [1*]Marcelino Montiel-Herrera [iD] .

[1]Departamento de Medicina y Ciencias de la Salud, Universidad de Sonora, Luis Donaldo Colosio s/n Edificio 7D, CP 83000, Hermosillo, Sonora, México. [2]Instituto Mexicano del Seguro Social. Hospital General de Zona 14. República de Cuba, El Mirasoles, CP 83120, Hermosillo, Sonora, México.

This article can be found at: https://eneurobiologia.uv.mx/index.php/eneurobiologia/article/view/2632

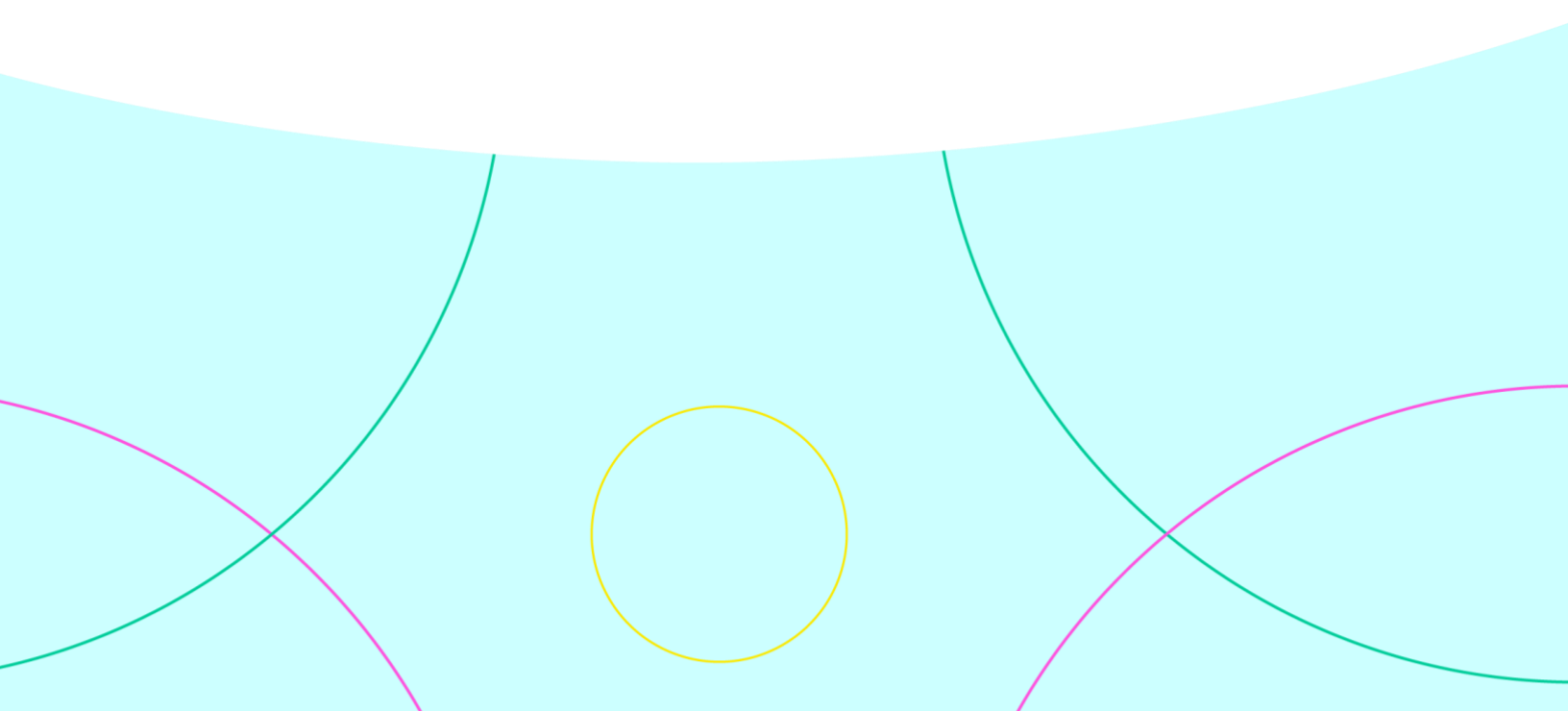*Corresponding author: Marcelino Montiel-Herrera. ORCID 0000-0002-8239-2356 e-mail address: marcelino.montiel@unison.mx. Departamento de Medicina y Ciencias de la Salud, Universidad de Sonora, Luis Donaldo Colosio s/n Edificio 7D, CP 83000, Hermosillo, Sonora, México.

Abstract

Glioblastoma multiforme is a lethal brain tumor. Experimental efforts to date have advanced our understanding of this tumor's pathophysiology. However, characterizing molecular targets is necessary to identify potential vulnerabilities and address its pathogenesis effectively. Here, we present excised glioblastoma multiforme brain tumors from two patients. We conducted *in situ* and *in vitro* Ca^{2+} imaging, end-point RT-PCR, and histological experiments to partially characterize the origin of intracellular Ca^{2+} responses in glioblastoma multiforme cells under diverse extracellular ionic and chemical-transmitter environments. These experimental approaches revealed that 70% of glioblastoma multiforme cells elicited spontaneous intracellular Ca^{2+} movements, among which 9% displayed rhythmic fluctuations, despite the absence of extracellular calcium and sodium. Moreover, IP3R and SERCA chemical antagonists were unable to completely inhibit these intracellular Ca^{2+} movements, while RT-PCR studies showed the expression of S100A9, KCNH1, SLC12A5, and SLC8A1. All these results suggest the participation of these proteins as part of the glioblastoma multiforme cell signaling machinery.

Keywords: Human, cancer, neurotransmitter, glial cells, intracellular calcium.

Resumen

El glioblastoma multiforme es un tumor cerebral letal. Los esfuerzos experimentales realizados hasta hoy han mejorado nuestra comprensión sobre la fisiopatología de dicho tumor. Sin embargo, es necesario encontrar objetivos moleculares para identificar vulnerabilidades potenciales y abordar su patogénesis eficientemente. Este trabajo estudió tumores cerebrales de glioblastoma multiforme extirpados de dos pacientes. A través de registros de Ca^{2+} intracelular *in situ* e *in vitro*, RT-PCR de punto final y experimentos histológicos se caracterizó parcialmente el origen de las respuestas de Ca^{2+} intracelular en células de glioblastoma multiforme humano expuestos a diversas concentraciones extracelulares iónicas y de transmisores químicos. Con ello se encontró que el 70% de las células de glioblastoma multiforme generaron movimientos espontáneos de Ca^{2+} intracelular, entre los cuales aproximadamente el 9% mostró fluctuaciones rítmicas, incluso en ausencia de calcio y sodio extracelular. Además, los antagonistas de IP3R y SERCA no inhibieron completamente las respuestas de Ca^{2+} intracelular, mientras que los estudios de RT-PCR mostraron la expresión de S100A9, KCNH1, SLC12A5 y SLC8A1. Estos resultados sugieren la participación de estas proteínas como parte de la maquinaria de señalización celular del glioblastoma multiforme.

Palabras clave: Humano, cáncer, neurotransmisores, células gliales, calcio intracelular.

1. Introduction

Glioblastoma multiforme (GBM) is a highly aggressive and deadly brain cancer, with a median survival time of less than two years.[1,2] Despite advances in treatment[3] the molecular mechanisms underlying GBM are not fully understood, and current therapies are often ineffective. Previous studies have identified ion channels and transporters as potential therapeutic targets for GBM[1], but their role in the development and progression of the disease is still not well understood. For instance, it is known that glioma cells intercommunicate through tumor microtubules via gap junctions to form functional multicellular networks within the brain. These tumor cell networks frequently use Ca^{2+} waves to communicate and are believed to participate in tumor network renewal after surgery, leading to tumor recurrence, and to resist other therapy approaches, such as chemotherapy and radiotherapy.[4] Nonetheless, complex multicellular patterns of Ca^{2+} activity are found in glioma tumor cells but their cellular origin and contribution to its pathophysiology are still unclear. Hence, due to its medical relevance, here we studied GBM samples of two patients and assessed the role of ion channels and transporters in its pathophysiology. Particularly, we monitored spontaneous and evoked intracellular Ca^{2+} movements (iCaM) in GBM cells using Fluo-4 AM imaging to study the contribution of extracellular Ca^{2+} ions and chemical-transmitters in the generation of these responses. Additionally, through end-point RT-PCR studies we investigated the expression of the ion transporters SLC8A1 and SLC12A5, the calcium-binding protein S100A9, and the potassium channel Kv10.1 in GBM cells, which are known to participate in cellular ion homeostasis. Our goal was to study GBM cell pathophysiology *in vitro* and to identify potential macromolecular targets that may lead to prognostic biomarkers for patients with this devastating disease.

2. Case presentation

Patient 1

A 57-year-old male presented with a 15-day history of bilateral weakness, predominantly affecting the lower limbs, along with marked gait impairment. Past medical history and remaining physical exam did not reveal any significant findings. A contrast-enhanced CT scan (Figure 1) revealed an ill-defined, heterogeneous, hypodense right temporal lesion with extension to ipsilateral basal nuclei, associated with partial collapse of the right ventricular system. The patient underwent craniotomy with excision of the lesion and postoperative histopathological examination confirmed primary GBM (WHO grade IV).
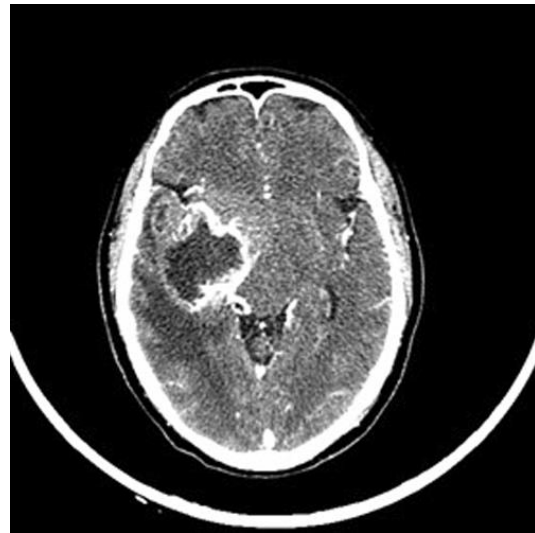
Figure 1. Contrast enhanced CT scan of intracranial tumor in the right temporal lobe prior to craniotomy.

Patient 2

A 64-year-old female presented with a 6-month history of memory deficits, headaches, loss of balance, and tremors involving hands and lips, followed by disorientation to space and time and

deviation of the left labial commissure one month prior to her admission. Three days preceding her admission, the patient presented with nystagmus, dysarthria, dysphagia, ataxic gait, and finally, sudden onset cognitive impairment. Upon her arrival, a physical examination revealed pale skin, perioral cyanosis, lethargy, bradylalia, anisocoric pupils with bilateral hypo-reactivity to light, and generalized weakness, predominantly of upper limbs. Medical history included untreated bipolar disorder. A head CT scan (Figure 2) revealed a heterogenous, hypo and hyperdense right temporal lesion with areas of necrosis associated with perilesional edema compressing the mesencephalon and ventricular system.

Figure 2. Simple CT scan of intracranial tumor in the right temporal lobe prior to craniotomy.

3. Materials and Methods

All methods were performed in accordance with relevant guidelines and regulations of the University of Sonora and approved by the Research Ethics Committee of the General Hospital of the State of Sonora, Hermosillo, Mexico (CEI 2022-39). Appropriate consents and permissions for publication were obtained, ensuring compliance with all relevant regulations and protocols.

Following excision, tumors and matched control samples (dura mater and cortex) were immediately placed in cold (4-8 °C) physiological artificial cerebrospinal fluid (aCSF) containing (in mM): 135 NaCl, 5.4 KCl, 1.8 $CaCl_2$, 1 $MgCl_2$, 5 HEPES, 10 glucose; pH adjusted to 7.4.

3.1 GBM primary cell cultures

GBM primary cell cultures were achieved following the method described by García-Carlos et al.[4] Human GBM cells were placed on poly-D-lysine-coated coverslips and cultures were kept at 37 °C with 5% CO_2 and 95% air. The culture medium was changed every third day over two weeks.

3.2 Ca^{2+} imaging experiments

From excised GBM tumors, we obtained GBM slices (400 µm thick) and performed Ca^{2+} imaging and end-point RT-PCR experiments. Additionally, GBM primary cell cultures (see below) were incubated in Petri dishes containing 10 µM Fluo-4 AM (Thermo Fisher Scientific, USA) diluted in aCSF for 10 min. GBM slices and cell cultures were fixed in a custom-made perfusion chamber positioned on a DM500 microscope platina (Leica Microsystems, USA). Specimens were perfused with physiological aCSF at a rate of 4 mL/min and visualized through a 20x/0.8 NA immersion objective (Leica Microsystems, USA). An X-cite XYLIS™ system (Excelitas technologies, USA) was applied to excite Fluo-4 (488 nm) with a LED intensity of 5%. The fluorescence emission (510 nm) was collected through a dichroic mirror. Frames were scanned and recorded at a rate of 2 frames/s during 10 min, using an Electro-Retiga CCD camera (Teledyne Photometrics, USA) with a resolution of 1376 x 1024 pixels. Baseline intracellular Ca^{2+} movements (iCaM) were represented by the fluorescence intensity ratio (%ΔF, arbitrary units, AU) and

were acquired through PVCAM software (Teledyne Photometrics, USA).

Following data acquisition, finite regions of interest of the frames were selected and analyzed with ImageJ 1.54g FIJI software (NIH, USA). iCaMs were depicted by Origin Pro 9.65 (OriginLab Corporation, Northampton, USA). Changes in fluorescence intensity are described as %ΔF and are displayed as mean ± standard error of n ≥ 25 cell recordings.

Via ion substitution, we recorded iCaM only in GBM cell cultures perfused with zero-Ca^{2+} aCSF (in mM: 135 NaCl, 5.4 KCl, 2.8 $MgCl_2$, 5 HEPES, 10 glucose; pH 7.4) and zero-Na^+ aCSF (in mM: 135 Choline-Cl, 5.4 KCl, 1.8 $CaCl_2$, 1 $MgCl_2$, 5 HEPES, 10 glucose; pH 7.4). Subsequently, to elucidate the role of K channels, GBM cells were alternatively perfused with 20 mM KCl, 1 µM $BaCl_2$ and, both 1 µM $BaCl_2$ + 20 mM KCl, dissolved in physiological, zero-Ca^{2+}, and zero-Na^{2+} aCSF.

GBM cell cultures were perfused with pharmacologic agents, 2-aminoethoxydiphenyl borate (50 µM 2-APB, cyclopiazonic acid (20 µM CPA), glutamate (1 mM), ATP (1 mM), angiotensin II (1 µM Ang II), and dopamine (1 mM). All reagents were obtained from Sigma-Aldrich unless indicated otherwise.

3.3 Immunofluorescence assay

In GBM cell cultures, immunofluorescence assays were carried out as described by Montiel-Herrera, et al.[5] In brief, following cell culture iCaM recording, cells were fixed in molecular grade methanol (≥99.9%) at -20 °C. At room temperature, primary rabbit anti-glial fibrillary acidic protein (anti-GFAP, 1:200; G9269, Sigma-Aldrich, USA) was used to incubate cells for 24 h and subsequently washed out 3 times with aCSF. Thereafter, cells were incubated with a secondary antibody, fluorescein isothiocyanate (FITC)-conjugated-goat antibody anti-rabbit IgG (1:300; F0382, Sigma Aldrich, USA) for 1 h. The samples were washed out as previously described and examined with an epifluorescence microscope for determining the percentage of immunoreactive cells. Control cells were treated with the secondary antibody alone. The latter did not fluoresce significantly. Assays were performed 3 times.

3.4 Histological analysis

GBM tissues were dehydrated, embedded in paraffin blocks, and 5 µm sections (n=12) were fixed onto glass slides. Eosin staining was performed, followed by a series of washes using 70/80/96% ethanol, absolute alcohol, and xylol. Slides were observed under an inverted Leica DM500 microscope (Leica Microsystems, USA) with a 40x objective lens. Images were captured using an Electro-Retiga CCD camera (Teledyne Photometrics, USA) with 1376 x 1024-pixel resolution. An area of 100 µm² was selected for each tissue section (n=12 slices from both samples) and masks were generated for cell count for the selected finite region of interest using ImageJ FIJI software (NIH, USA). This procedure was used only to confirm the general characteristics GBM tumors.[6]

3.5 Reverse transcription-polymerase chain reaction (RT-PCR)

Total RNA (tRNA) extraction of GBM tissues and their matched control tissue was performed using Direct-zol RNA MiniPrep according to the manufacturer's instructions (Zymo Research), followed by reverse transcription (RT) carried out using the GoScript reverse transcription system (Promega). Both tRNA and RT were quantified using a Nanodrop apparatus (Thermo Fisher, USA). Amplification of cDNA was achieved by end-point PCR using a MiniAmp Thermal Cycler (Applied Biosystems) and visualized using agarose gel electrophoresis. All products are the result of ≥2 repetitions. Primer sequences and amplicons are shown in Table 1.

Primer	Sequence 5' to 3' (forward, reverse)	Amplicon	NCBI ID
S100A9	CTCCTCGGCTTTGACAGAGTG CAGCTGCTTGTCTGCATTTGT	250 bp	NM_002965.4
KCNH1	AACGTGGATGAGGGCATCAG GTACAGCCAGCTGTTGTTGC	240 bp	NM_002238.4
SLC12A5	AAAAAGAAGCCGGTGCAGGC CACCATGCAGAAGGACTCCA	147 bp	NM_001134771.2
SLC8A1	GCGGCGATTAAGTCTTTCAC TTGTTCCCAAAAGAAGGGTC	162 bp	NM_021097.5
β-actin	TCGTGCGTGACATTAAAGAG TGCCACAGGATTCCATAC	198 bp	NM_031144.3

Table 1. Experimental oligonucleotide sequences. Sequences were confirmed using Basic Local Alignments Search Tool (NIH).

4. Data analysis

All data obtained from intracellular Ca^{2+} recordings in GBM cells were analyzed with descriptive statistics and are given as mean ± standard error of n ≥ 25 cells, unless indicated otherwise. End-point RT-PCR data were obtained from at least 2 replicas.

5. Results

The histological analysis confirmed general characteristic of human GBM tumor (not shown).[6] Based on the immunofluorescence assays conducted in GBM cells, over 95% of recorded cells were positive to GFAP.

5.1 GBM cells show spontaneous intracellular Ca^{2+} movements (iCaM)

In situ Ca^{2+} imaging experiments carried out in GBM slices from both samples perfused with physiological aCSF, zero-Ca^{2+} and zero-Na^{1+} revealed spontaneous iCaM (Figure 3). Of 142 GBM cells recorded, 70% presented at least one iCaM among which, roughly 9% demonstrated rhythmic fluctuations (Figure 3A). Under physiologic aCSF, 24/65 GBM cells presented at least one spontaneous iCaM, 38/86 in zero-Ca^{2+}, and 26/33 in zero-Na^{1+}. Furthermore, 71 of 142 GBM cells exposed to 20 mM K^{1+} under physiologic aCSF presented iCaM.
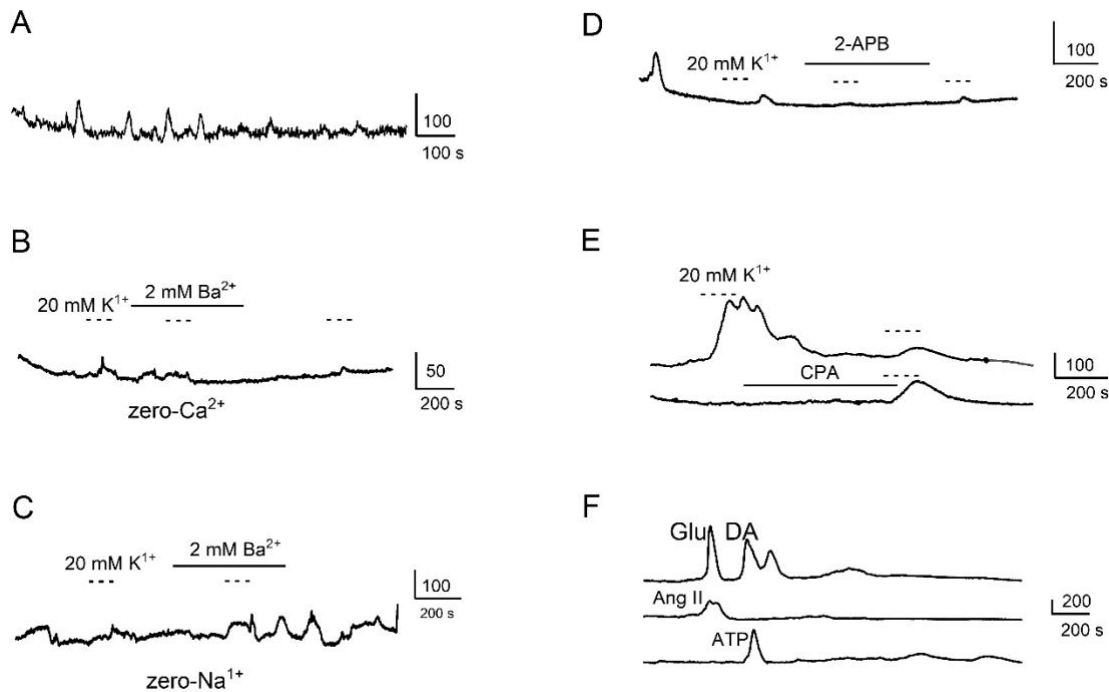
Figure 3. Human glioblastoma multiforme cell intracellular Ca^{2+} movements. A, spontaneous intracellular Ca^{2+} movements (iCaM); B-C, effect of Potassium and Barium ions on iCaM; D-E, effect of 2-APB and CPA on iCaM; F, evoked iCaM by Glu, glutamate, DA, dopamine, Ang II, Angiotensin II, and ATP, adenosine triphosphate.

Primary cell cultures exposed to 20 mM K^{1+} produced similar iCaM when perfused with physiologic aCSF and in the absence of extracellular Ca^{2+} (26%, n=27, and 24%, n=78, respectively). Among responses generated with zero-Ca^{2+} + 20 mM K^{1+} aCSF, 11% (n=78) displayed rhythmic fluctuations. Notably, iCaM were increased when extracellular Na^{1+} was removed (55%, n=29). Additionally, the aCSF perfusion containing 1 µM Ba^{2+} + 20 mM K^{1+}, zero-Ca^{2+} (Figure 3B), and zero-Na^{1+} (Figure 3C) evoked iCaM in 11% (n=27), 22% (n=78), and 35% (n=26) cells, respectively.

Furthermore, we assessed the intracellular signaling mechanisms associated with iCaM in cultured GBM cells. Upon inhibition of inositol 1,4,5-trisphosphate receptor (IP3R) using 2-APB, we continued to observe iCaM activity in GBM cells (76% of cells, n=71; Figure 3D).

However, iCaM were reduced in GBM cells upon inhibition of the sarcolemma-endoplasmic reticulum Ca^{2+}-ATPase (SERCA) by CPA in 12% of cells (n=73; Figure 3E).

5.2 Neurotransmitters evoke iCaM in GBM cells

GBM cells responded to 1 mM glutamate, 1 mM ATP, 1 µM Ang II, and 1 mM dopamine with iCaM (Figure 3F). Glutamate elicited responses in 9% (n=348) of cells, while ATP prompted responses in a lower percentage, with 6% (n=348) of cells. Ang II, on the other hand, induced responses in 5% (n=348) of cells, suggesting relatively limited cellular responsiveness to these chemical transmitters. In contrast, dopamine exerted a major number of iCaM (26% of cells, n=348) of outward oscillatory characteristics.

5.3 mRNA expression

End-point RT-PCR was performed to determine if differences existed between GBM samples and matched non-neoplastic tissue (dura mater and cortex). We found the expression of all amplicons studied, including ion transporters Na/Ca (SLC8A1) and K/Cl (SLC12A5), the K channel Kv10.1 (KCNH1; HERG), and the calcium-binding protein S100A9, present in all 4 tissues (Figure 4).
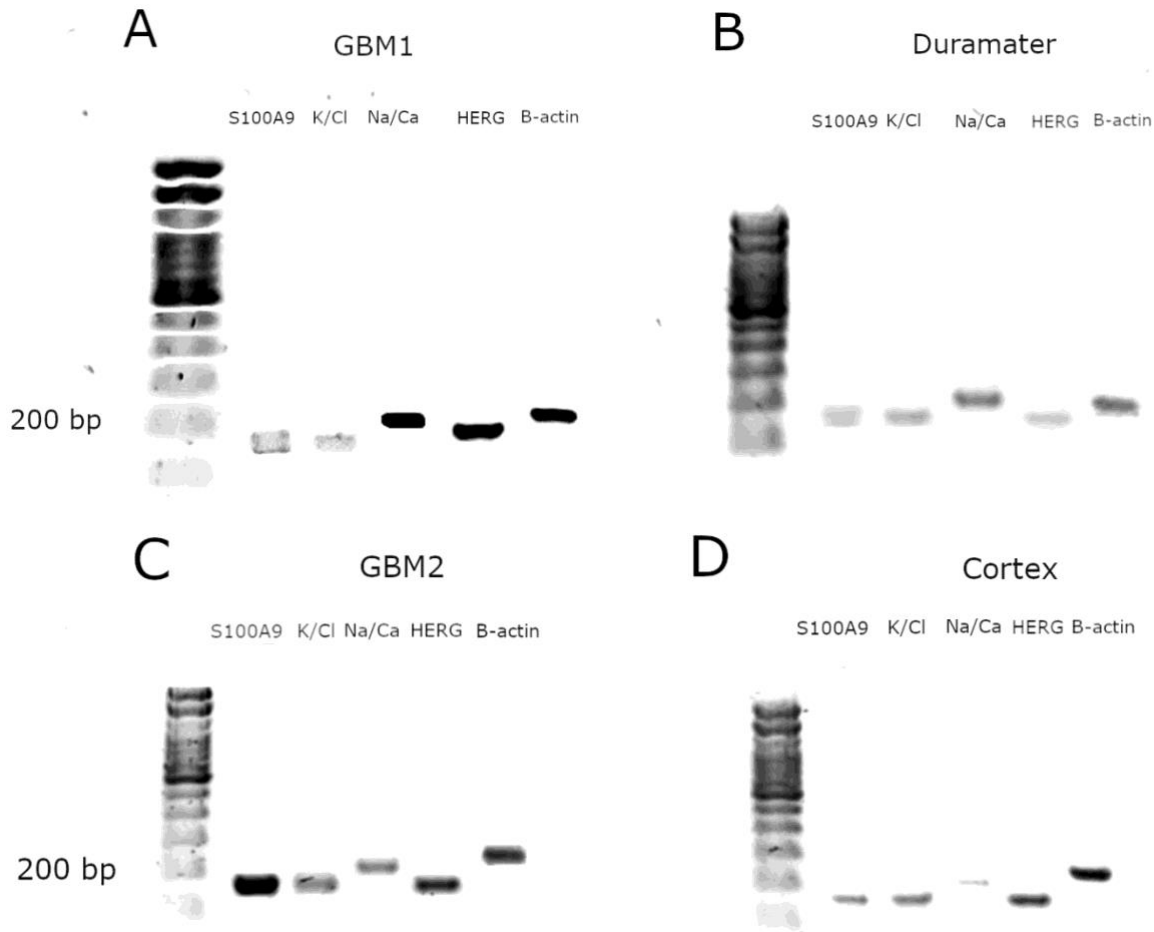
Figure 4. Endpoint RT-PCR amplicons of GBM 1 (A) and GBM 2 (B) with matched controls.

6. Discussion

In glial cells, electrochemical gradients, extracellular agonists, mechanical stretch, and intracellular chemical messengers evoke transient intracellular Ca^{2+} fluctuations regulated by specialized machinery which allow Ca^{2+} cytoplasmic accumulation, storage, and release.[7] This signaling machinery includes ion channels, exchangers, pumps, and binding proteins found in cell and organelle membranes.[8] Each of these present potential vulnerabilities that could be targeted to combat and ultimately overcome the pathology of GBM cells.[9] iCaM occur at distinct spatial and temporal levels along cells, which are in turn decoded into intrinsic functional effects or transmitted to

adjacent cells.[10,11] Therefore, the specific characteristics of GBM cells could be determined by variations in both the type and quantity of the signaling machinery they possess.[9]

Evidence suggests that aberrant intracellular Ca^{2+} signaling may play a critical role in the pathogenesis of GBM by promoting tumor growth, migration, and resistance to therapy.[12] The mechanisms underlying the generation and regulation of these Ca^{2+} oscillations are not well understood. Here, we used *in situ* and *in vitro* Ca^{2+} imaging, along with molecular biology techniques, to partially characterize the nature of iCaM in GBM cells in response to different extracellular ionic and chemical-transmitter environments.

As recently found, we also discovered the presence of rhythmic iCaM in GBM samples. This autonomic activity is known to trigger KCa3.1 and subsequent downstream activation of MAPK and NF-κB pathways.[9] In our study, the rhythmic and overall Ca^{2+} oscillations were attenuated when exposed to Ba^{2+} (in physiologic and zero-Ca^{2+} aCSF), a time- and voltage-dependent inhibitor of the human ether-à-go-go related gene (HERG).[13] Both HERG and KCa3.1 have shown to be upregulated in GBM and attributed to its invasive characteristics.[13,14]

Alike previous studies performed on GBM and colorectal carcinoma cell lines, elimination of extracellular Ca^{2+} influx does not abolish spontaneous iCaMs, suggesting that internal stores have an important role in cytosolic Ca^{2+} concentrations.[15,16] Li et al. (2020) reported that these Ca^{2+} transients were present for up to 1-2 h following withdrawal of extracellular Ca^{2+} but were eliminated after 4 h.[15] Interestingly, we observed a higher percentage of cells generating iCaMs in the absence of extracellular Ca^{2+} and Na^{1+} ions compared to physiological aCSF. These findings raise several intriguing questions about the mechanisms underlying these oscillations that merit further research.

Li et al. (2020) demonstrated that GBM cells can reach unusually high Ca^{2+} concentrations (3-5 µM) without triggering cell death, possibly mediated by overexpression of mitochondrial Ca^{2+} uniporter (MCU).[15] Silencing this mitochondrial Ca^{2+} uniporter causes a decrease in spontaneous Ca^{2+} fluctuations, but does not entirely eliminate them, implying additional internal stores contribute to cytosolic Ca^{2+} oscillations. To investigate this, we perfused GBM cultures with 2-APB, a selective inhibitor of IP3R-mediated Ca^{2+} release[17], expressed primarily in the endoplasmic reticulum and Golgi apparatus. We found that 75% of GBM cells (n=71) continued to evoke spontaneous iCaMs despite IP3R inhibition, indicating that distinct mechanisms may be used for Ca^{2+} signaling. In contrast, previous studies have reported that inhibition of IP3R significantly inhibits rises in intracellular Ca^{2+} in GBM cell lines and inhibits *in vivo* tumor growth of colon and prostate cancer cells.[16,18] Additionally, we found that the inhibition of SERCA by CPA[19] significantly reduced the amount of GBM cells producing iCaM. SERCA is known to contribute to free Ca^{2+} clearance and to increase cytosolic Ca^{2+} via interaction with stromal interacting molecule (STIM1) adaptor protein.[20] STIM1 directly interacts with Orai1, a pore forming unit of the store-operated Ca^{2+} and has previously been implicated in GBM cell invasion.[21] These studies, along with our findings, may indicate that GBM cells may use the SERCA-STIM1/Orai1 complex for generating iCaM; however, it is important to note that this mechanism is not the sole contributor of iCaM production, as iCaMs were not completely eliminated despite all experimental conditions used.

In physiological aCSF, the presence of Na^{1+} allows for normal functioning of Na^{+1}-

dependent ion transporters, such as the Na/Ca exchanger, Na/K ATPase, and Na/Cl/K cotransporter. When Na^{+1} is removed from the extracellular solution, it disrupts the activity of these Na^{+1}-dependent ion transporters, specifically the Na/Ca exchanger, which normally helps remove excess Ca^{2+} from the cell. Without Na^{+1}, the exchanger's activity may be compromised, leading to impaired Ca^{2+} extrusion and subsequent accumulation. These results are supported by findings showing that blocking the reverse mode of the Na/Ca exchanger does not affect tumor growth, while suppressing the forward mode suppresses human GBM cell lines.[22] Although other factors may be participating in the aggressiveness of GBM cells associated with iCaM triggered by biomechanical forces[23–25] that merit further research. In this context, it was surprising that a small percentage of GBM cells responded with iCaM in response to common transmitters like glutamate, ATP, and Ang II, in comparison to dopamine. Dopamine signaling has garnered growing attention as a target of interest in GBM tumorigenesis and may play an interesting role in the pathogenesis of GBM. Lower levels of DRD1 expression in GBM human samples and experimental models have been associated with shorter median survival times and increased cell viability, respectively.[26] Similar to our study, Yang et al (2020) demonstrated that DRD1 agonists increase fluorescent intensity in Fluo 4-loaded GBM cells, and concurrent DRD1 knockdown prevents its increase. Upon Ca^{2+} chelation by BAPTA, the effect of DRD1 agonists on GBM cells was partially inhibited, leading to improved cell viability.[26] This leads to the assumption that the increased iCaM evoked by dopamine in our study may be attributed to DRD1 activation, potentially triggering either PKA or PLC/IP3 signaling pathways, and ultimately leading to cell death. In addition to dopamine, we tested glutamate, ATP, and Ang II. While all three elicited comparable responses among themselves, dopamine differed from them in terms of inducing more iCaM and exhibiting an inverted bell-shaped amplitude.

With the goal to identify possible molecular targets on GBM cells, we investigated through end-point RT-PCR the expression of the ion transporters Na/Ca and K/Cl, the K channel Kv10.1, and the calcium-binding protein S100A9. Although the expression of all amplicons studied were present in GBM samples and matched control tissues, GBM amplicon products appeared to be expressed with greater intensity compared to control. Nonetheless further experiments are required to properly quantify significant differences between samples. Of interest, the S100 proteins regulate cellular responses following the detection of intracellular Ca^{2+} changes and have been described to participate in GBM proliferation and invasion.[27,28] We identified S100A9 mRNA in both tumor and matched control tissues. S100A9 has been reported to be over-expressed in tumor-infiltrating myeloid-derived cells and plasma from glioma patients rather than the tumor itself.[29,30] Neurons can also release S100A9 (in conjunction with S100A8), resulting in Kras-induced gliosis and microglia recruitment.[31] Nonetheless, S100A9 has been found to be strongly up regulated in GBM stem cells.[32] By exerting inhibitory effects on telomerase activity and thereby enhancing cellular immortality,[8] these Ca^{2+} binding proteins strengthen the notion that non-neoplastic cells, such as the dura mater and cortex beforementioned, may actively participate in shaping a tumor-permissive microenvironment through the release of S100A9.

In pursuit of a better understanding of the Ca^{2+} signaling heterogeneity observed in GBM cells, future research should prioritize functional validation. This is paramount to establishing causal relationships between identified channels and the observed cellular responses. Conducting targeted knockdown or overexpression studies in GBM-animal models will enable researchers to manipulate the expression levels of specific molecular entities and assess their impact on calcium dynamics.

7. Acknowledgments

8. Funding

9. Statements and declarations

All the authors declare that they have no known competing financial interests or personal relationships that could have appeared to influence the work reported in this paper.

10. Data Availability Statement

The data that support the findings of this study are available from the corresponding author upon reasonable request.

11. References

1. Wang H-Y, Li J-Y, Liu X, Yan X-Y, Wang W, Wu F, Liang T-Y, Yang F, Hu H-M, Mao H-X, Liu Y-W, Zhang S-Z. A three ion channel genes-based signature predicts prognosis of primary glioblastoma patients and reveals a chemotherapy sensitive subtype. Oncotarget 2016; 7: 74895–903.

2. Weller M, Wick W, Aldape K, Brada M, Berger M, Pfister SM, Nishikawa R, Rosenthal M, Wen PY, Stupp R, Reifenberger G. Glioma. Nat Rev Dis Primer 2015; 1: 15017.

3. Ling AL, Solomon IH, Landivar AM, Nakashima H, Woods JK, Santos A, Masud N, Fell G, Mo X, Yilmaz AS, Grant J, Zhang A, Bernstock JD, Torio E, Ito H, Liu J, Shono N, Nowicki MO, Triggs D, Halloran P, Piranlioglu R, Soni H, Stopa B, Bi WL, Peruzzi P, Chen E, Malinowski SW, Prabhu MC, Zeng Y, Carlisle A, Rodig SJ, Wen PY, Lee EQ, Nayak L, Chukwueke U, Gonzalez Castro LN, Dumont SD, Batchelor T, Kittelberger K, Tikhonova E, Miheecheva N, Tabakov D, Shin N, Gorbacheva A, Shumskiy A, Frenkel F, Aguilar-Cordova E, Aguilar LK, Krisky D, Wechuck J, Manzanera A, Matheny C, Tak PP, Barone F, Kovarsky D, Tirosh I, Suvà ML, Wucherpfennig KW, Ligon K, Reardon DA, Chiocca EA. Clinical trial links oncolytic immunoactivation to survival in glioblastoma. Nature 2023; 623: 157–66.

4. García-Carlos CA, Camargo-Loaiza JA, García-Villa D, López-Cervantes JG, Domínguez-Avila JA, González-Aguilar GA, Astiazaran-Garcia H, Montiel-Herrera M. Angiotensin II, ATP and high extracellular potassium induced intracellular calcium responses in primary rat brain endothelial cell cultures. Cell Biochem Funct 2021; 39: 688–98.

5. Montiel-Herrera M, Miledi R, García-Colunga J. Membrane currents elicited by angiotensin II in astrocytes from the rat corpus callosum. Glia 2006; 53: 366–71.

6. Urbańska K, Sokołowska J, Szmidt M, Sysa P. Review Glioblastoma multiforme – an overview. Współczesna Onkol 2014; 5: 307–12.

7. Verkhratsky A, Orkand RK, Kettenmann H. Glial Calcium: Homeostasis and Signaling Function. Physiol Rev 1998; 78: 99–141.

8. Bruce JIE, James AD. Targeting the Calcium Signalling Machinery in Cancer. Cancers 2020; 12: 2351.

9. Hausmann D, Hoffmann DC, Venkataramani V, Jung E, Horschitz S, Tetzlaff SK, Jabali A, Hai L, Kessler T, Azořin DD, Weil S, Kourtesakis A, Sievers P, Habel A, Breckwoldt MO, Karreman MA, Ratliff M, Messmer JM, Yang Y, Reyhan E, Wendler S, Löb C, Mayer C, Figarella K, Osswald M, Solecki G, Sahm F, Garaschuk O, Kuner T, Koch P, Schlesner M, Wick W, Winkler F. Autonomous rhythmic activity in glioma networks drives brain tumour growth. Nature 2023; 613: 179–86.

10. Scemes E, Giaume C. Astrocyte calcium waves: What they are and what they do. Glia 2006; 54: 716–25.

11. Bazargani N, Attwell D. Astrocyte calcium signaling: the third wave. Nat Neurosci 2016; 19: 182–9.

12. Maklad A, Sharma A, Azimi I. Calcium Signaling in Brain Cancers: Roles and Therapeutic Targeting. Cancers 2019; 11: 145.

13. Weerapura M, Nattel S, Courtemanche M, Doern D, Ethier N, Hebert T. State-dependent barium block of wild-type and inactivation-deficient HERG channels in Xenopus oocytes. J Physiol 2000; 526 Pt 2: 265–78.

14. Jehle J, Schweizer PA, Katus HA, Thomas D. Novel roles for hERG K+ channels in cell proliferation and apoptosis. Cell Death Dis 2011; 2: e193–e193.

15. Li X, Spelat R, Bartolini A, Cesselli D, Ius T, Skrap M, Caponnetto F, Manini I, Yang Y, Torre V. Mechanisms of malignancy in glioblastoma cells are linked to mitochondrial Ca2+ uniporter upregulation and higher intracellular Ca2+ levels. J Cell Sci 2020; 133: jcs237503.

16. Liang C, Zhang Q, Chen X, Liu J, Tanaka M, Wang S, Lepler SE, Jin Z, Siemann DW, Zeng B, Tang X. Human cancer cells generate spontaneous calcium transients and intercellular waves that modulate tumor growth. Biomaterials 2022; 290: 121823.

17. Peppiatt CM, Collins TJ, Mackenzie L, Conway SJ, Holmes AB, Bootman MD, Berridge MJ, Seo JT, Roderick HL. 2-Aminoethoxydiphenyl borate (2-APB) antagonises inositol 1,4,5-trisphosphate-induced calcium release, inhibits calcium pumps and has a use-dependent and slowly reversible action on store-operated calcium entry channels. Cell Calcium 2003; 34: 97–108.

18. Kang SS, Han K-S, Ku BM, Lee YK, Hong J, Shin HY, Almonte AG, Woo DH, Brat DJ, Hwang EM, Yoo SH, Chung CK, Park S-H, Paek SH, Roh EJ, Lee S joong, Park J-Y, Traynelis SF, Lee CJ. Inhibition of the Ca2+ release channel, IP3R subtype 3 by caffeine slows glioblastoma invasion and migration and extends survival. Cancer Res 2010; 70: 1173–83.

19. Moncoq K, Trieber CA, Young HS. The Molecular Basis for Cyclopiazonic Acid Inhibition of the Sarcoplasmic Reticulum Calcium Pump. J Biol Chem 2007; 282: 9748–57.

20. Serwach K, Gruszczynska-Biegala J. Target Molecules of STIM Proteins in the Central Nervous System. Front Mol Neurosci 2020; 13: 617422.

21. Motiani RK, Hyzinski-García MC, Zhang X, Henkel MM, Abdullaev IF, Kuo Y-H, Matrougui K, Mongin AA, Trebak M. STIM1 and Orai1 Mediate CRAC Channel Activity and are Essential for Human Glioblastoma Invasion. Pflugers Arch 2013; 465: 1249–60.

22. Hu H-J, Wang S-S, Wang Y-X, Liu Y, Feng X-M, Shen Y, Zhu L, Chen H-Z, Song M. Blockade of the forward Na+ /Ca2+ exchanger suppresses the growth of glioblastoma cells through Ca2+ -

mediated cell death. Br J Pharmacol 2019; 176: 2691–707.

23. Grossen A, Smith K, Coulibaly N, Arbuckle B, Evans A, Wilhelm S, Jones K, Dunn I, Towner R, Wu D, Kim Y-T, Battiste J. Physical Forces in Glioblastoma Migration: A Systematic Review. Int J Mol Sci 2022; 23: 4055.

24. Pontes B, Mendes FA. Mechanical Properties of Glioblastoma: Perspectives for YAP/TAZ Signaling Pathway and Beyond. Diseases 2023; 11: 86.

25. Wang X, Gong Z, Wang T, Law J, Chen X, Wanggou S, Wang J, Ying B, Francisco M, Dong W, Xiong Y, Fan JJ, MacLeod G, Angers S, Li X, Dirks PB, Liu X, Huang X, Sun Y. Mechanical nanosurgery of chemoresistant glioblastoma using magnetically controlled carbon nanotubes. Sci Adv 2023; 9: eade5321.

26. Yang K, Wei M, Yang Z, Fu Z, Xu R, Cheng C, Chen X, Chen S, Dammer E, Le W. Activation of dopamine receptor D1 inhibits glioblastoma tumorigenicity by regulating autophagic activity. Cell Oncol Dordr 2020; 43: 1175–90.

27. Arora A, Patil V, Kundu P, Kondaiah P, Hegde AS, Arivazhagan A, Santosh V, Pal D, Somasundaram K. Serum biomarkers identification by iTRAQ and verification by MRM: S100A8/S100A9 levels predict tumor-stroma involvement and prognosis in Glioblastoma. Sci Rep 2019; 9: 2749.

28. Wang H, Mao X, Ye L, Cheng H, Dai X. The Role of the S100 Protein Family in Glioma. J Cancer 2022; 13: 3022.

29. Gautam P, Nair SC, Gupta MK, Sharma R, Polisetty RV, Uppin MS, Sundaram C, Puligopu AK, Ankathi P, Purohit AK, Chandak GR, Harsha HC, Sirdeshmukh R. Proteins with Altered Levels in Plasma from Glioblastoma Patients as Revealed by iTRAQ-Based Quantitative Proteomic Analysis. PLoS ONE 2012; 7: e46153.

30. Gielen PR, Schulte BM, Kers-Rebel ED, Verrijp K, Bossman SAJFH, ter Laan M, Wesseling P, Adema GJ. Elevated levels of polymorphonuclear myeloid-derived suppressor cells in patients with glioblastoma highly express S100A8/9 and arginase and suppress T cell function. Neuro-Oncol 2016; 18: 1253–64.

31. Ryu M-J, Liu Y, Zhong X, Du J, Peterson N, Kong G, Li H, Wang J, Salamat S, Chang Q, Zhang J. Oncogenic Kras expression in postmitotic neurons leads to S100A8-S100A9 protein overexpression and gliosis. J Biol Chem 2012; 287: 22948–58.

32. Chen S, Zhao H, Deng J, Liao P, Xu Z, Cheng Y. Comparative proteomics of glioma stem cells and differentiated tumor cells identifies S100A9 as a potential therapeutic target. J Cell Biochem 2013; 114: 2795–808.